Polymer Journal (2018) 50:177–186
https://doi.org/10.1038/s41428-017-0006-6

ORIGINAL ARTICLE

Gas transport properties of polybenzoxazole–silica hybrid membranes prepared with different alkoxysilanes

Tomoyuki Suzuki[1] · Yusuke Otsuki[1]

Received: 14 July 2017 / Revised: 16 October 2017 / Accepted: 20 October 2017 / Published online: 7 December 2017

Abstract

The gas transport properties of polybenzoxazole (PBO)–silica hybrid membranes were investigated. The PBO–silica hybrid membranes were prepared with poly(*o*-hydroxy amide) (PHA) as a precursor and various alkoxysilanes via thermal oxazolization and sol–gel processes. The thermal decomposition temperature of the hybrid membranes increased with increasing silica content, indicating that the thermal stability was improved by hybridization with silica. The gas permeabilities of the PBO–silica hybrid membranes also increased with increasing silica content and thermal treatment temperature. It is worth noting that the hybrid membranes prepared with tetraethoxysilane (TEOS) as the selected alkoxysilane showed simultaneous enhancements in CO_2 permeability and CO_2/CH_4 selectivity with increasing silica content and thermal treatment temperature. The prominent CO_2/CH_4 separation ability of the PBO–silica hybrid membranes prepared with TEOS might be attributable to free volume holes created around the polymer/silica interfacial area and increased intermolecular chain distance, which improved size-selective CO_2/CH_4 separation.

Introduction

Gas separation using polymeric membranes has markedly attracted attention during the past several decades [1–3]. Compared to conventional separation processes such as pressure-swing adsorption, chemical absorption, and cryogenic distillation, membrane-based gas separation is advantageous because of its low capital and operating costs, high energy efficiency, and ease of operation [4–6]. In this regard, a large number of polymeric membranes have been developed to achieve high gas permeation and separation abilities. Polyimides (PIs) [7–10]. and polybenzoxazoles (PBOs) [11–13]. classified as rigid-rod aromatic polymers are promising materials for high-performance gas separation membranes because of their high gas permselectivities and high thermal and mechanical properties. Recently, Pinnau and coworkers have shown that intrinsically microporous, triptycene-based PIs with a large fractional free volume and a well-defined free volume architecture have great potential as high-performance gas separation membranes [14–16]. On the other hand, it has been reported that thermally rearranged PBOs, named TR-PBOs, show extraordinarily high gas permselectivities owing to their high fractional free volume and the intrinsic size and distribution of their free volume holes [6,17–21].

Another approach, hybridization with inorganic compounds, has also been emphasized as a method for modifying PIs and PBOs to improve their gas transport properties [4,22–24]. In our previous study, it has been found PI–silica hybrid membranes prepared via a sol–gel reaction with several alkoxysilane species possess controlled gas permselectivity, suggesting that free volume holes created around the polymer/silica interfacial area can be tuned to achieve a desired gas permselectivity [25]. Additionally, PBO–silica hybrid membranes prepared with tetraethoxysilane (TEOS) as the selected alkoxysilane have shown improved CO_2/CH_4 selectivity [26]. To date, however, there are no experimental reports on the gas transport properties of PBO–silica hybrid membranes prepared with different kinds of alkoxysilanes.

In the present work, PBO–silica hybrid membranes were prepared with different alkoxysilane species via a sol–gel process, and their gas transport properties were investigated. During membrane preparation, several thermal treatment temperatures were examined. It has been revealed that

✉ Tomoyuki Suzuki
suzuki@kit.ac.jp

[1] Faculty of Materials Science and Engineering, Kyoto Institute of Technology, Matsugasaki, Sakyo-ku, Kyoto 606-8585, Japan

increasing the treatment temperature results in PBOs with improved gas permeability owing to the increased interchain distance and fractional free volume [11, 27]. With the simultaneous application of hybridization and thermal treatment techniques, the preparation of PBO-based high-performance gas separation membranes with attractive gas permeability and/or selectivity would be expected.

Experimental procedures

Materials

2,2-Bis(3-amino-4-hydroxyphenyl)hexafluoropropane (6FAHP), 4,4'-oxybis(benzoic acid chloride) (OBC), TEOS, and phenyltrimethoxysilane (PhTMS) were purchased from Tokyo Chemical Industry Co., Ltd. (Tokyo, Japan). *N,O*-Bis(trimethylsilyl)acetamide (BSA), an amide-type silylation agent, was obtained from Sigma-Aldrich Japan (Tokyo, Japan). 3-(Triethoxysilyl)propylsuccinic anhydride (TEOSPSA), a coupling agent, and *N,N*-dimethylacetamide (DMAc), a solvent, were supplied by AZmax Co. (Tokyo, Japan) and Nacalai Tesque, Inc. (Kyoto, Japan), respectively. These regents and solvent were used as received. Chemical structures of the monomers are shown in Fig. 1.

Polymerization

As a precursor, poly(*o*-hydroxy amide) (PHA) was synthesized by the in situ silylation method described as follows [28, 29]: 5 mmol of 6FAHP was dissolved in 10 ml of DMAc in a 50 ml three-neck flask under N_2 flow. Next, 20 mmol of BSA was added to this solution with stirring at room temperature, and the solution was continually stirred for 1 h. Then, the solution was cooled in an ice-ethanol bath at 0–5 °C, and 4.85 mmol of OBC was added with stirring. The mixture was kept stirring at 0–5 °C for 1 h and then at room temperature for 3 h under N_2 flow. The resulting polymer solution was poured into distilled water. The precipitated polymer was collected and washed thoroughly with distilled water, followed by vacuum drying at 90 °C for 4 h. Finally, amine-terminated 6FAHP-OBC poly(*o*-hydroxy amide), PHA(6FAHP-OBC) was obtained as a solid polymer. A schematic representation of the synthesis of PHA(6FAHP-OBC) is shown in Fig. 2.

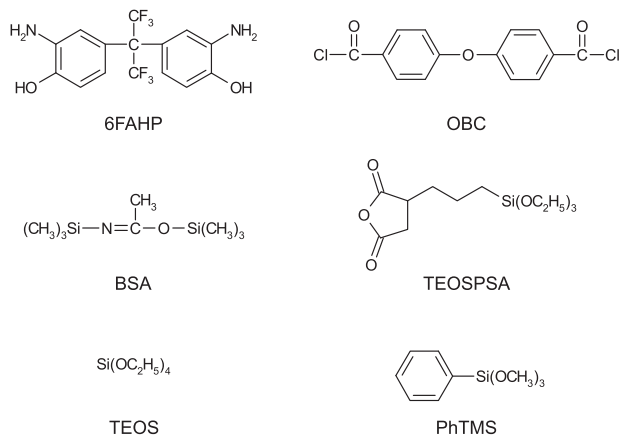

Fig. 1 Chemical structures of the monomers

Membrane formation

PHA(6FAHP-OBC) (0.5 g) was dissolved in 5 ml of DMAc, and 0.050 g of TEOSPSA was added with stirring. To this solution, appropriate amounts of a selected alkoxysilane, TEOS or PhTMS, and distilled water and a catalytic amount of diluted hydrochloric acid were added, and the reaction mixture was stirred overnight. The preparation conditions of the corresponding reaction mixtures are summarized in Table 1. Next, the mixture was cast on a PET sheet and dried at 85 °C for 1 h in a heating oven to form a thin membrane. The prepared membrane was peeled off, fixed between two window-opened metal frames, and then dehydrocyclized and hybridized by subsequent stepwise heating in a heating oven under N_2 flow: (a) 100 °C for 1 h, (b) 200 °C for 1 h, and (c) a selected temperature of 400, 420, or 450 °C for 1 h. Finally, 6FAHP-OBC polybenzoxazole (PBO(6FAHP-OBC))–silica (SiO_2) hybrid membranes were obtained. Because our previous work demonstrated that the thermal decomposition of pristine PBO(6FAHP-OBC) initiated at ~470 °C[26]. the upper limit of the thermal treatment temperature was set to 450 °C.

Here, the hybrid membranes prepared with TEOS or PhTMS are denoted PBO(6FAHP-OBC)–SiO_2 (TEOS) and PBO(6FAHP-OBC)–SiO_2 (PhTMS), respectively.

Measurements

Attenuated total reflection Fourier transform infrared (ATR FT-IR) spectra were recorded by an FT/IR-4100 equipped with an ATR PRO ONE (ZnSe prism) (JASCO Corp., Japan) at a wavenumber range of 550–4000 per cm and a resolution of 2 per cm. Scanning electron microscopy (SEM) images were acquired using an S-3400N variable pressure SEM (Hitachi High-Technologies Corp., Japan) at an accelerating voltage of 10 kV. Samples for the SEM analyses were coated using an E-1010 ion sputter coater (Hitachi High-Technologies Corp., Japan) with a platinum target. Differential scanning calorimetry (DSC) measurements were carried out with a DSC-60 (Shimadzu Corp., Japan) at a heating rate of 10 °C/min and a temperature range of 25–400 °C under N_2 flow. Thermogravimetric–differential thermal analysis (TG–DTA) experiments were performed with a DTG-60 (Shimadzu Corp., Japan) at a

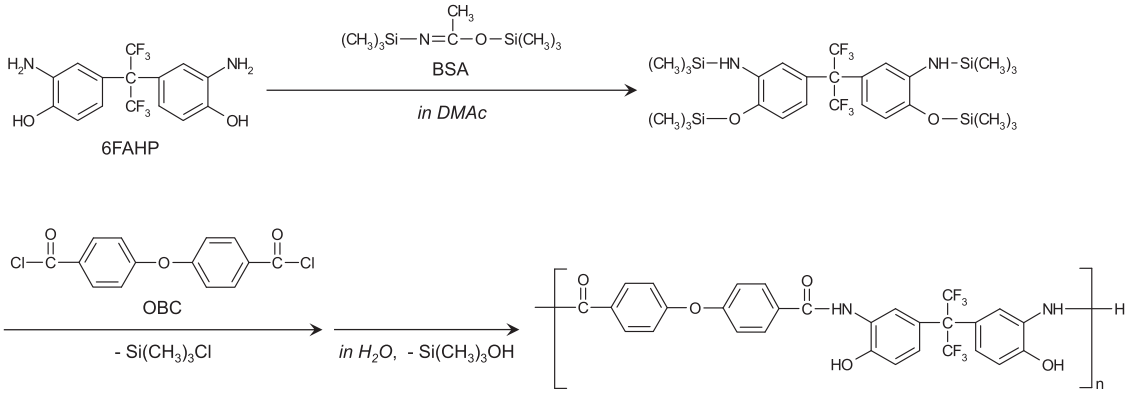

Fig. 2 Schematic representation of the synthesis of PHA(6FAHP-OBC)

heating rate of 10 °C/min and a temperature range of 25–800 °C under air flow. CO_2, O_2, N_2, and CH_4 permeation measurements were carried out with a constant volume/variable pressure apparatus at 76 cmHg and 25 °C. The permeability coefficient, P (barrer, 1 barrer $= 1 \times 10^{-10}$ cm^3(STP) cm/cm^{2}s cmHg), was determined by the following equation [30]:

$$P = \left[\frac{273}{T} \cdot \frac{V}{A} \cdot L \cdot \frac{1}{p} \cdot \frac{1}{76} \cdot \frac{\mathrm{d}p}{\mathrm{d}t}\right] \times 10^{10} \quad (1)$$

where T is the absolute temperature (K), V is the downstream volume (cm^3), A is the membrane area (cm^2), L is the membrane thickness (cm), p is the upstream pressure (cmHg), and dp/dt is the permeation rate (cmHg/s). The gas permeability coefficient can be explained on the basis of the solution-diffusion mechanism, which is represented by the following equation [31, 32]:

$$P = D \times S \quad (2)$$

where D (cm^2/s) is the diffusion coefficient and S (cm^3 (STP)/cm$^3_{\text{polym.}}$ cmHg) is the solubility coefficient. The diffusion coefficient was calculated by the time-lag method represented by the following equation [33]:

$$D = \frac{L^2}{6t} \quad (3)$$

where t (s) is the time-lag. Wide-angle X-ray scattering (WAXS) patterns were recorded by an MX-Labo (Mac Science Co., Ltd.) using Cu-Kα radiation with a wavelength of $\lambda = 1.54$ Å. The scan range was from 10 to 25° under a voltage of 40 kV and a current of 18 mA. The average d-spacing, d(Å), was determined based on Bragg's law [27]:

$$n\lambda = 2d \sin\theta \quad (4)$$

where n is an integer, λ denotes the X-ray wavelength, and θ indicates the diffraction angle. A floating method was used for measuring the densities of pristine PBO(6FAHP-OBC) membranes prepared by different thermal protocols with NaBr aqueous solution at 25 °C. According to the group contribution method, the fractional free volume (FFV) of a polymer can be estimated by the following equations [34, 35]:

$$\mathrm{FFV} = \frac{V_{\mathrm{sp}} - 1.3V_{\mathrm{w}}}{V_{\mathrm{sp}}} \quad (5)$$

$$V_{\mathrm{sp}} = \frac{M}{\rho} \quad (6)$$

where V_{sp} (cm^3/mol) is the specific molar volume, V_{w} (cm^3/mol) is the van der Waals volume of the repeating unit, M (g/mol) is the molecular weight of the repeating unit, and ρ (g/cm^3) is the experimental density.

Results and discussion

Membrane characterization

Figure 3 shows ATR FT-IR spectra of PHA(6FAHP-OBC), PBO(6FAHP-OBC), and silica hybrid membranes (SiO_2 content: 30 wt%). For PHA(6FAHP-OBC), the bands assigned to the amide linkage are found at ~1540 (N–H bending) and 1650 per cm (C=O stretching) [27, 36]. On the other hand, for PBO(6FAHP-OBC), the bands attributed to the amide linkage mentioned above disappeared, and new absorption bands appeared at 1052 (phenyl–O–C stretching), 1480 (benzoxazole ring), and 1612 per cm (C=N stretching), which are characteristic bands of PBO [12, 18, 27, 37, 38]. This finding indicates that PHA(6FAHP-OBC) is successfully converted into PBO(6FAHP-OBC) by the established thermal treatment protocol. For the hybrid membranes PBO(6FAHP-OBC)–SiO_2 (TEOS) and SiO_2 (PhTMS) (SiO_2 content: 30 wt%), a strong absorption band at ~1000–1200 per cm assigned to Si–O–Si asymmetric stretching [39, 40]. is also observed. Additionally, for PBO (6FAHP-OBC)–SiO_2 (PhTMS), the absorption band at 697 per cm (out-of-plane deformation of phenyl groups) is

Table 1 Preparation condition of the PBO(6FAHP-OBC)–silica hybrid membranes

Polymer (g)	TEOSPSA (g)	Required SiO_2 content (wt%)	TEOS (g)	PhTMS (g)	H_2O (g)
0.5	0.050	0	–	–	–
		10	0.212	–	0.110
		20	0.477	–	0.248
		30	0.818	–	0.424
		10	–	0.202	0.083
		20	–	0.454	0.186
		30	–	0.779	0.318

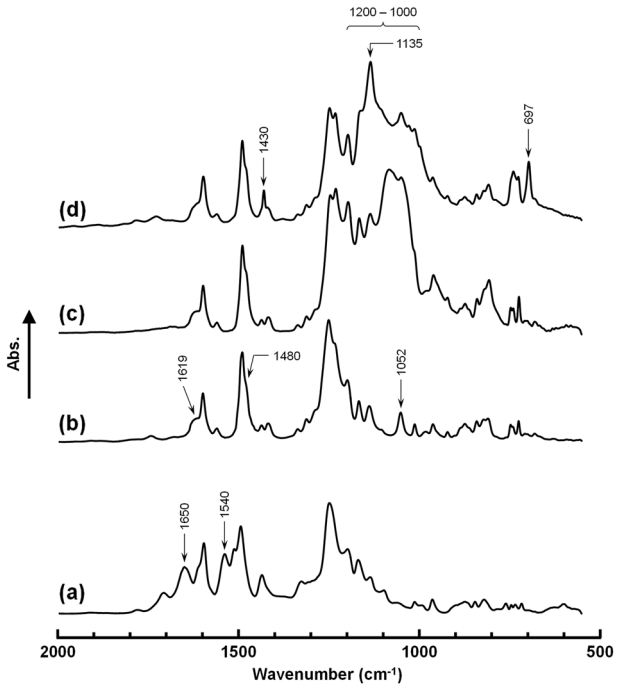

Fig. 3 ATR FT-IR spectra of **a** PHA(6FAHP-OBC), **b** PBO(6FAHP-OBC), **c** PBO(6FAHP-OBC)–SiO_2 (TEOS) (SiO_2 content: 30 wt%), and **d** PBO(6FAHP-OBC)–SiO_2 (PhTMS) (SiO_2 content: 30 wt%); **b**–**d** are prepared at 400 °C

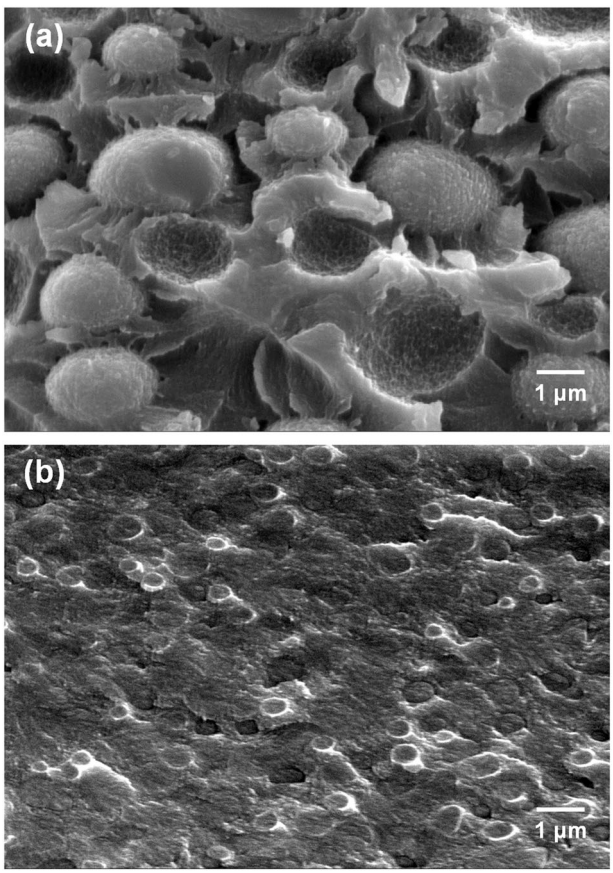

Fig. 4 Cross-sectional SEM images of **a** PBO(6FAHP-OBC)–SiO_2 (TEOS) (SiO_2 content: 30 wt%) and **b** PBO(6FAHP-OBC)–SiO_2 (PhTMS) (SiO_2 content: 30 wt%) prepared at 400 °C

observed, together with bands at 1135 and 1430 per cm related to Si–phenyl deformation [39, 41]. These results confirm that the sol–gel reaction occurs during the membrane preparation process and that the expected Si–O–Si network structures are formed in the PBO(6FAHP-OBC)–SiO_2 (TEOS) and SiO_2 (PhTMS) hybrid membranes.

Figure 4 presents cross-sectional SEM images of PBO(6FAHP-OBC)–SiO_2 (TEOS) and SiO_2 (PhTMS) (SiO_2 content: 30 wt%). PBO(6FAHP-OBC)–SiO_2 (TEOS) has a rugged cross-sectional morphology because of the approximately 1–3 μm of aggregated silica domains (Fig. 4a). On the other hand, PBO(6FAHP-OBC)–SiO_2 (PhTMS) in Fig. 4b shows smaller and more dispersed silica domains than PBO(6FAHP-OBC)–SiO_2 (TEOS). The small and well-dispersed silica domains in PBO(6FAHP-OBC)–SiO_2 (PhTMS) might result from the phenyl substituent of the PhTMS moiety. The phenyl substituent might function as an inhibitor of the formation of the Si–O–Si network during the sol–gel process, resulting in suppressed aggregation of the silica domains. In addition, the phenyl substituent would also improve the affinity for the PBO matrix, leading to well-dispersed silica domains.

The thermal properties of the hybrid membranes were investigated by DSC and TG–DTA measurements. Glass transition temperatures (T_gs) and 5% weight-loss temperatures (T_d^5s) of the hybrid membranes are listed in Table 2, in addition to the silica contents determined from the residual

Table 2 Thermal properties of the PBO(6FAHP-OBC)–silica hybrid membranes prepared at 400 °C

Sample	T_g (°C)	T_d^5 in air (°C)	Residual at 800 °C (wt%)
PBO(6FAHP-OBC)	308	512	–
SiO_2 (TEOS) = 10 wt%	312	514	13
SiO_2 (TEOS) = 20 wt%	313	520	21
SiO_2 (TEOS) = 30 wt%	314	527	32
SiO_2 (PhTMS) = 10 wt%	302	516	10
SiO_2 (PhTMS) = 20 wt%	300	520	20
SiO_2 (PhTMS) = 30 wt%	300	525	27

Table 3 Gas transport properties, *d*-spacing, and FFV of the PBO(6FAHP-OBC)–silica hybrid membranes at 25 °C

Preparation temperature (°C)	Alkoxysilane	SiO_2 content (wt%)	P (Barrer)				$D \times 10^8$ (cm^2/s)				$S \times 10^2$ (cm^3(STP)/$cm^3_{polym.}$ cmHg)				*d*-spacing (Å)	FFV	Ref.
			CO_2	O_2	N_2	CH_4	CO_2	O_2	N_2	CH_4	CO_2	O_2	N_2	CH_4			
400	–	0	68	12	2.3	1.7	2.4	6.8	1.6	0.32	29	1.8	1.4	5.3	6.14	0.182	[26]
	TEOS	10	103	18	3.5	2.5	3.6	9.1	2.2	0.45	29	2.0	1.6	5.6			[26]
		20	168	29	6.2	4.2	5.0	15	4.0	0.71	34	2.0	1.6	5.7			[26]
		30	206	34	6.9	4.2	6.4	18	4.4	0.83	32	1.9	1.6	5.1			[26]
	PhTMS	10	145	22	5.4	5.6	6.7	15	5.4	1.2	22	1.5	1.0	4.6			
		20	158	23	5.7	7.1	8.7	17	6.6	1.8	18	1.3	0.86	3.9			
		30	222	30	7.9	11	12	21	8.4	2.8	17	1.4	0.94	4.0			
420	–	0	109	19	3.9	2.9	3.7	8.9	2.2	0.43	29	2.2	1.8	6.6	6.23	0.184	
	TEOS	10	162	28	6.0	4.5	5.7	14	3.6	0.73	28	2.0	1.7	6.2			
		20	224	37	8.1	5.5	6.4	15	4.6	0.84	35	2.4	1.7	6.5			
		30	340	53	12	7.5	9.6	23	6.5	1.2	35	2.3	1.8	6.3			
	PhTMS	10	191	28	6.7	5.9	6.0	13	4.3	0.87	32	2.2	1.6	6.7			
		20	347	49	12	14	14	26	11	2.5	25	1.9	1.2	5.1			
		30	552	78	20	21	26	43	18	4.1	22	1.8	1.1	5.0			
450	–	0	529	85	20	14	10	29	8.1	1.1	52	2.9	2.5	13	6.50	0.185	
	TEOS	10	583	86	20	14	11	29	7.9	1.3	52	3.0	2.5	11			
		20	942	126	32	22	17	38	10	1.8	55	3.3	3.0	12			
	PhTMS	10	984	145	41	41	21	48	17	4.0	48	3.0	2.4	10			
		20	1248	174	49	57	27	63	21	5.8	47	2.8	2.3	9.9			

mass at 800 °C. As expected, all the hybrid membranes are confirmed to contain appropriate amounts of silica. The T_d^5s of the hybrid membranes increase with increasing silica content. This result indicates that hybridization with silica increases the thermal stability of the PBO matrix. The PBO (6FAHP-OBC)–SiO_2 (TEOS) hybrid membranes show higher T_gs than pristine PBO(6FAHP-OBC), suggesting the formation of a robust three-dimensional Si–O–Si network. On the other hand, the PBO(6FAHP-OBC)–SiO_2 (PhTMS) hybrid membranes show lower T_gs than PBO(6FAHP-OBC). This result suggests that phenyl substituent of the PhTMS moiety leads to insufficient formation of the Si–O–Si network and effective disruption of molecular chain packing[25, 42], which decreases the constraint of molecular chains in the hybrid membranes.

Gas transport properties

The gas permeability, diffusion, and solubility coefficients of the PBO(6FAHP-OBC)–silica hybrid membranes prepared with different alkoxysilanes and thermal treatment protocols are summarized in Table 3. Unfortunately, we could not carry out gas permeation measurements for the 450 °C-treated hybrid membranes containing 30 wt% of silica due to shrinkage-induced breakage of the membranes during the cooling process of membrane formation. First, from the perspective of the effect of hybridization with silica, it should be noted that the gas permeability of the hybrid membranes increases with increasing silica content, mainly in conjunction with increased gas diffusivity. Similar enhancements of gas permeability and/or diffusivity

have been reported by Merkel et al. for high free volume, glassy polymer-nanosized silica composites, and they have concluded the silica particles yield a polymer/particle interfacial area and provide disruption of polymer chain packing, that affects the gas transport behavior [43, 44]. In another study on positron annihilation lifetime spectroscopy analyses of PI-based mixed matrix membranes (MMMs), it has been determined that the incorporation of inorganic nanoparticles accelerates the formation of additional free volume holes, which leads to increased gas diffusivity and, as a consequence, increased gas permeability of the MMMs [45]. Therefore, the increased gas permeability attributed to the increased gas diffusivity of the PBO(6FAHP-OBC)–silica membranes might be caused by the formation of free volume holes around the polymer/silica interfacial area. Notably, the gas permeability and diffusivity of PBO (6FAHP-OBC)–SiO_2 (PhTMS) are higher than those of PBO(6FAHP-OBC)–SiO_2 (TEOS). The more enhanced permeability and diffusivity of PBO(6FAHP-OBC)–SiO_2 (PhTMS) are considered to be due to formation of free volume holes around the polymer/silica interfacial area facilitated by the phenyl substituent of the PhTMS moiety. It has also been revealed that adding surface-modified silica nanoparticles into a polymer matrix facilitates the formation of nanogaps between nanoparticles and polymer chain segments [46, 47]. As presented in Fig. 4b, compared to PBO(6FAHP-OBC)–SiO_2 (TEOS), PBO (6FAHP-OBC)–SiO_2 (PhTMS) features small and well-dispersed silica domains, which in turn can increase the polymer/silica interfacial area and thus would also

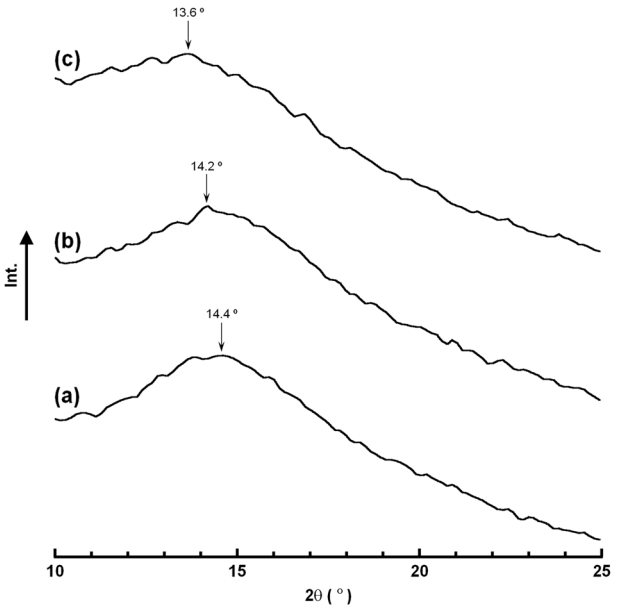

Fig. 5 WAXS patterns of pristine PBO(6FAHP-OBC)s prepared at **a** 400 °C, **b** 420 °C, and **c** 450 °C

Table 4 O_2/N_2 and CO_2/CH_4 selectivities of the PBO(6FAHP-OBC)–silica hybrid membranes at 25 °C

Preparation temperature (°C)	Alkoxysilane	SiO_2 content (wt%)	O_2/N_2 separation			CO_2/CH_4 separation			Ref.
			$\alpha(O_2/N_2)$	$\alpha^D(O_2/N_2)$	$\alpha^S(O_2/N_2)$	$\alpha(CO_2/CH_4)$	$\alpha^D(CO_2/CH_4)$	$\alpha^S(CO_2/CH_4)$	
400	–	0	5.4	4.2	1.3	40	7.3	5.5	[26]
	TEOS	10	5.3	4.1	1.3	41	8.0	5.1	[26]
		20	4.6	3.7	1.3	41	7.0	5.9	[26]
		30	4.9	4.1	1.2	49	7.8	6.2	[26]
	PhTMS	10	4.1	2.7	1.5	26	5.5	4.7	
		20	4.0	2.6	1.6	22	4.7	4.7	
		30	3.8	2.5	1.4	20	4.5	4.5	
420	–	0	5.1	4.1	1.3	38	8.7	4.4	
	TEOS	10	4.7	3.8	1.2	36	7.8	4.6	
		20	4.6	3.3	1.4	41	7.6	5.4	
		30	4.5	3.5	1.3	45	8.0	5.7	
	PhTMS	10	4.2	3.0	1.5	33	6.9	4.7	
		20	3.9	2.6	1.5	27	4.8	4.7	
		30	3.9	2.4	1.6	27	6.2	4.3	
450	–	0	4.3	3.7	1.2	37	9.1	4.1	
	TEOS	10	4.3	3.6	1.2	42	9.0	4.6	
		20	4.0	3.6	1.1	44	9.7	4.5	
	PhTMS	10	3.6	2.8	1.3	24	5.1	4.7	
		20	3.6	3.0	1.2	22	4.8	4.6	

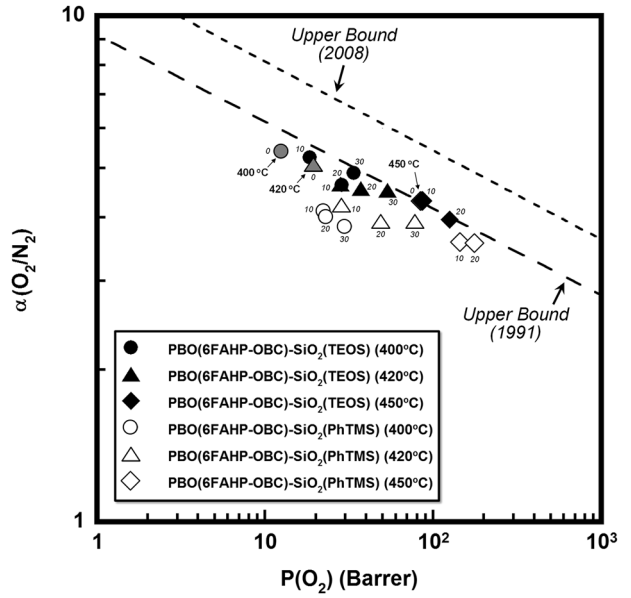

Fig. 6 Ideal O_2/N_2 selectivity of PBO(6FAHP-OBC)–SiO_2 (TEOS) (filled symbols) and PBO(6FAHP-OBC)–SiO_2 (PhTMS) (unfilled symbols) plotted against the O_2 permeability coefficient measured at 25 °C; the attached number represents the SiO_2 content (wt%) in the membrane

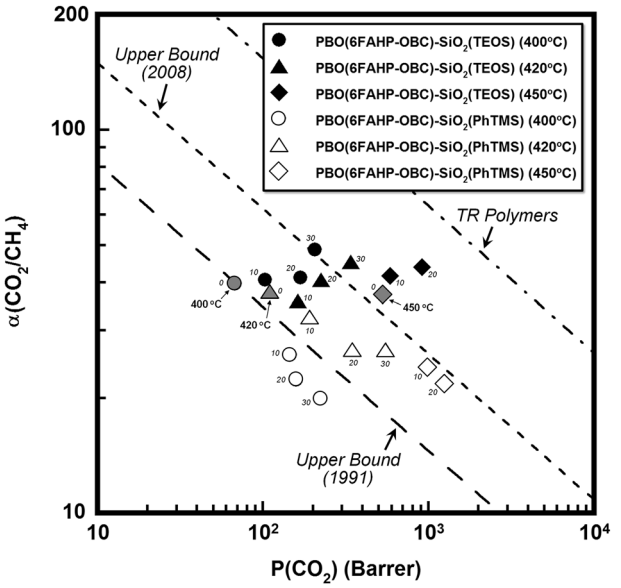

Fig. 7 Ideal CO_2/CH_4 selectivity of PBO(6FAHP-OBC)–SiO_2 (TEOS) (filled symbols) and PBO(6FAHP-OBC)–SiO_2 (PhTMS) (unfilled symbols) plotted against the CO_2 permeability coefficient measured at 25 °C; the attached number represents the SiO_2 content (wt%) in the membrane

contribute to the higher gas permeability and diffusivity of PBO(6FAHP-OBC)–SiO_2 (PhTMS).

The thermal treatment temperature also affects to gas transport properties of pristine PBO(6FAHP-OBC) and its silica hybrid membranes. As shown in Table 3, the gas permeability and diffusivity of PBO(6FAHP-OBC) and its silica hybrid membranes increase with increasing thermal treatment temperature. Figure 5 presents WAXS patterns of pristine PBO(6FAHP-OBC) membranes prepared with different thermal treatment protocols, and *d*-spacing values calculated from Eq. (4) are listed in Table 3 together with *FFV* values obtained from Eqs. (5) and (6). Both the *d*-spacing attributed to intermolecular chain distance and *FFV* increase with increasing thermal treatment temperature. Wang et al. have reported that for a PBO membrane, increased treatment temperature causes increases in inter-chain distance and free volume radius, which lead to enhanced gas permeabilities [11, 27]. The improved gas permeability and diffusivity of PBO (6FAHP-OBC) and its silica hybrid membranes by increased treatment temperature are therefore attributed to the increased intermolecular chain distance and *FFV*. Especially for the hybrid membranes, the gas permeability and diffusivity are efficiently improved by the effects of both hybridization with silica and increased treatment temperature.

The ideal gas selectivity for the combination of gases A and B (α(A/B)) is defined by the following equation [48]:

$$\alpha(\mathrm{A/B}) = \frac{P(\mathrm{A})}{P(\mathrm{B})} = \frac{D(\mathrm{A})}{D(\mathrm{B})} \times \frac{S(\mathrm{A})}{S(\mathrm{B})} = \alpha^D(\mathrm{A/B}) \times \alpha^S(\mathrm{A/B}) \quad (7)$$

where α^D(A/B) is the diffusivity selectivity and α^S(A/B) is the solubility selectivity. The O_2/N_2 and CO_2/CH_4 selectivities of the PBO(6FAHP-OBC)–silica hybrid membranes are listed in Table 4. It is found that the ideal selectivity (α(A/B)) for a given gas pair essentially depends on the diffusivity selectivity (α^D(A/B)) rather than the solubility selectivity (α^S(A/B)), which is consistent with a general understanding of the gas separation behavior of glassy polymers [48]. The obtained $\alpha(O_2/N_2)$ and $\alpha(CO_2/CH_4)$ values are plotted against the O_2 and CO_2 permeability coefficients in Figs. 6 and 7, respectively. In Fig. 6, the α (O_2/N_2) values slightly decrease with increasing O_2 permeability, along with the upper bound trade-off line for O_2/N_2 separation demonstrated by Robeson in 1991 [49]. This behavior is consistent with the general trend that glassy polymers that are more permeable are less selective, and vice versa [48]. Nevertheless, it can be seen that the PBO (6FAHP-OBC)–silica hybrid membranes have a favorable O_2/N_2 separation ability because they show relatively high α (O_2/N_2) values just below the upper bound presented in 1991.

For CO_2/CH_4 separation, interesting behaviors are observed. As shown in Fig. 7, the $\alpha(CO_2/CH_4)$ of the PBO (6FAHP-OBC)–SiO_2 (TEOS) increases with increasing CO_2 permeability with a tendency to cross the upper bound for CO_2/CH_4 separation [49, 50]. Considering the difference in kinetic diameter between CO_2 (3.3 Å) and CH_4 (3.87 Å) [48], the improved CO_2/CH_4 separation ability of PBO (6FAHP-OBC)–SiO_2 (TEOS) might be due to characteristic

free volume holes around the polymer/silica interfacial area that improve size-selective CO_2/CH_4 separation. On the other hand, the $\alpha(CO_2/CH_4)$ of the PBO(6FAHP-OBC)–SiO_2 (PhTMS) monotonically decreases, in conjunction with decreased $\alpha^D(CO_2/CH_4)$ (Table 4), with increasing CO_2 permeability along with the upper bound. The distinctive difference between PBO(6FAHP-OBC)–SiO_2 (TEOS) and PBO(6FAHP-OBC)–SiO_2 (PhTMS) may be due to the differences in the mean size and total amount of free volume holes created around the polymer/silica interfacial area. The size-selective CO_2/CH_4 separation ability of PBO(6FAHP-OBC)–SiO_2 (PhTMS) is sacrificed by excess increases in the mean size and total amount of free volume holes caused by the phenyl substituent of the PhTMS moiety, whereas the overall gas permeability is markedly increased owing to increased gas diffusivity.

It should be mentioned that PBO(6FAHP-OBC) and its silica hybrid membranes maintain fundamental CO_2/CH_4 separation behavior, whereas their CO_2 permeability is highly accelerated with increasing treatment temperature. In particular, 450 °C-treated PBO(6FAHP-OBC)–SiO_2 (TEOS) possesses an excellent CO_2/CH_4 separation ability that exceeds the upper bound updated in 2008. This prominent CO_2/CH_4 separation ability might be attributable to the simultaneous effects of (1) characteristic free volume holes created around the polymer/silica interfacial area caused by the hybridization with TEOS-induced silica and (2) enhanced intermolecular chain distance and free volume holes due to the thermal treatment, which improves size-selective CO_2/CH_4 separation. Even though 450 °C-treated PBO(6FAHP-OBC)–SiO_2 (TEOS) cannot exceed the advanced trade-off line of CO_2/CH_4 separation for existing TR-polymers, including TR-PBOs (Fig. 7)[17, 50, 51]. the PBO(6FAHP-OBC)–silica hybrid membranes have an attractive CO_2/CH_4 separation ability that can be tailored to specific requirements by altering the alkoxysilane species and the thermal treatment temperature.

Conclusions

The gas transport properties of PBO(6FAHP-OBC)–silica hybrid membranes prepared by applying different alkoxysilane species and thermal treatment protocols were investigated. The thermal decomposition temperatures of the PBO(6FAHP-OBC)–SiO_2 (TEOS) and SiO_2 (PhTMS) hybrid membranes increase with increasing silica content, indicating that hybridization with silica improves the thermal stability. The gas permeability of the PBO(6FAHP-OBC)–silica hybrid membranes also increases with increasing silica content, suggesting the formation of free volume holes around the polymer/silica interfacial area. For PBO(6FAHP-OBC)–SiO_2 (PhTMS), a more enhanced permeability is observed, which might be attributed to the formation of free volume holes induced by the phenyl substituent of the PhTMS moiety. The gas permeability of the PBO(6FAHP-OBC)–silica hybrid membranes is further increased with increasing thermal treatment temperature owing to the increased intermolecular chain distance and FFV. In particular, 450 characteristic free volume holes created around the polymer/silica interfacial area caused by the hybridization with TEOS-induced silica and [2]. enhanced intermolecular chain distance and free volume holes due to the thermal treatment, which improves size-selective CO_2/CH_4 separation. With the simultaneous application of hybridization and thermal treatment techniques, the development of PBO-based high-performance gas separation membranes with attractive gas permeability and/or selectivity would be expected.

Acknowledgements This work was supported by JSPS KAKENHI Grant Number 17K05994.

Compliance with ethical standards

Conflict of interest The authors declare that they have no competing interests.

References

1. Bernardo P, Drioli E, Golemme G. Membrane gas separation: a review/state of the art. Ind Eng Chem Res. 2009;48:4638–63.
2. Brunetti A, Scura F, Barbieri G, Drioli E. Membrane technologies for CO_2 separation. J Membr Sci. 2010;359:115–25.
3. Robeson LM, Smith ZP, Freeman BD, Paul DR. Contributions of diffusion and solubility selectivity to the upper bound analysis for glassy gas separation membranes. J Membr Sci. 2014;453:71–83.
4. Chung TS, Jiang LY, Li Y, Kulprathipanja S. Mixed matrix membranes (MMMs) comprising organic polymers with dispersed inorganic fillers for gas separation. Prog Polym Sci. 2007;32:483–507.
5. Zhang Y, Sunarso J, Liu S, Wang R. Current status and development of membranes for CO_2/CH_4 separation: a review. Int J Greenh Gas Control 2013;12:84–107.
6. Calle M, Doherty CM, Hill AJ, Lee YM. Cross-linked thermally rearranged poly(benzoxazole-co-imide) membranes for gas separation. Macromolecules 2013;46:8179–89.
7. Langsman M, Burgoyne WF. Effect of diamine monomer structure on the gas permeability of polyimides. I. Bridged diamines. J Polym Sci A Polym Chem. 1993;31:909–21.
8. Li Y, Wang X, Ding M, Xu J. Effect of molecular structure on the permeability and permselectivity of aromatic polyimides. J Appl Polym Sci 1996;61:741–8.
9. Suzuki T, Yamada Y, Tsujita Y. Gas transport properties of 6FDA-TAPOB hyperbranched polyimide membrane. Polymer. 2004;45:7167–71.
10. Kammakakam I, Yoon HW, Nam SY, Park HB. Novel piperazinium-mediated crosslinked polyimide membranes for high performance CO_2 separation. J Membr Sci. 2015;487:90–8.

11. Wang H, Liu S, Chung TS, Chen H, Jean YC, Pramoda KP. The evolution of poly(hydroxyamide amic acid) to poly(benzoxazole) via stepwise thermal cyclization: structural changes and gas transport properties. Polymer. 2011;52:5127–38.
12. Yeong YF, Wang H, Pramoda KP, Chung TS. Thermal induced structural rearrangement of cardo-copolybenzoxazole membranes for enhanced gas transport properties. J Membr Sci. 2012;397-8:51–65.
13. Jo HJ, Soo CY, Dong G, Do YS, Wang HH, Lee MJ, Quay JR, Murphy MK, Lee YM. Thermally rearranged poly(benzoxazole-co-imide) membranes with superior mechanical strength for gas separation obtained by tuning chain rigidity. Macromolecules. 2015;48:2194–202.
14. Ghanem BS, Swaidan R, Litwiller E, Pinnau I. Ultra-microporous triptycene-based polyimide membranes for high-performance gas separation. Adv Mater. 2014;26:3688–92.
15. Swaidan R, Ghanem B, Litwiller E, Pinnau I. Effects of hydroxyl-functionalization and sub-T_g thermal annealing on high pressure pure-and mixed-gas CO_2/CH_4 separation by polyimide membranes based on 6FDA and triptycene-containing dianhydrides. J Membr Sci. 2015;475:571–81.
16. Ghanem B, Alghunaimi F, Ma X, Alaslai N, Pinnau I. Synthesis and characterization of novel triptycene dianhydrides and polyimides of intrinsic microporosity based on 3,3'-dimethylnaphthidine. Polymer. 2016;101:225–32.
17. Park HB, Jung CH, Lee YM, Hill AJ, Pas SJ, Mudie ST, Wagner EV, Freeman BD, Cookson DJ. Polymers with cavities tuned for fast selective transport of small molecules and ions. Science. 2007;318:254–8.
18. Calle M, Lee YM. Thermally rearranged (TR) poly(ether-benzoxazole) membranes for gas separation. Macromolecules. 2011;44:1156–65.
19. Sanders DF, Guo R, Smith ZP, Liu Q, Stevens KA, McGrath JE, Paul DR, Freeman BD. Influence of polyimide precursor synthesis route and ortho-position functional group on thermally rearranged (TR) polymer properties: conversion and free volume. Polymer. 2014;55:1636–47.
20. Liu Q, Paul DR, Freeman BD. Gas permeation and mechanical properties of thermally rearranged (TR) copolyimides. Polymer. 2016;82:378–91.
21. Woo KT, Lee J, Dong G, Kim JS, Do YS, Jo HJ, Lee YM. Thermally rearranged poly(benzoxazole-co-imide) hollow fiber membranes for CO_2 capture. J Membr Sci. 2016;498:125–34.
22. Cornelius CJ, Marand E. Hybrid silica-polyimide composite membranes: gas transport properties. J Membr Sci. 2002;202:97–118.
23. Jusoh N, Yeong YF, Lau KK, Shariff AM. Enhanced gas separation performance using mixed matrix membranes containing zeolite T and 6FDA-durene polyimide. J Membr Sci. 2017;525:175–86.
24. Wijenayake SN, Panapitiya NP, Versteeg SH, Nguyen CN, Goel S, Balkus KJ Jr, Musselman IH, Ferraris JP. Surface cross-linking of ZIF-8/polyimide mixed matrix membranes (MMMs) for gas separation. Ind Eng Chem Res. 2013;52:6991–7001.
25. Suzuki T, Yamada Y, Itahashi K. 6FDA-TAPOB hyperbranched polyimide-silica hybrids for gas separation membranes. J Appl Polym Sci. 2008;109:813–9.
26. Suzuki T, Takenaka M, Yamada Y. Synthesis and gas transport properties of hyperbranched polybenzoxazole–silica hybrid membranes. J Membr Sci. 2017;521:10–17.
27. Wang H, Chung TS. The evolution of physicochemical and gas transport properties of thermally rearranged polyhydroxyamide (PHA). J Membr Sci. 2011;385–386:86–95.
28. Imai Y, Itoya K, Kakimoto M. Synthesis of aromatic polybenzoxazoles by silylation method and their thermal and mechanical properties. Macromol Chem Phys. 2000;201:2251–6.
29. Oishi Y, Konno A, Oravec J, Mori K. Synthesis and properties of fluorine-containing polybenzoxazoles by in situ silylation method. J Photopolym Sci Technol. 2006;19:669–72.
30. Miyata S, Sato S, Nagai K, Nakagawa T, Kudo K. Relationship between gas transport properties and fractional free volume determined from dielectric constant in polyimide films containing the hexafluoroisopropylidene group. J Appl Polym Sci. 2008;107:3933–44.
31. Muruganandam N, Koros WJ, Paul DR. Gas sorption and transport in substituted polycarbonates. J Polym Sci B Polym Phys. 1987;25:1999–2026.
32. Morisato A, Shen HC, Sankar SS, Freeman BD, Pinnau I, Casillas CG. Polymer characterization and gas permeability of poly(1-trimethylsilyl-1-propyne) [PTMSP], poly(1-phenyl-1-propyne) [PPP], and PTMSP/PPP blends. J Polym Sci B Polym Phys. 1996;34:2209–22.
33. Weinkauf DH, Kim HD, Paul DR. Gas transport properties of liquid crystalline poly(p-phenyleneterephthalamide). Macromolecules 1992;25:788–96.
34. van Krevelen DW. Properties of Polymers. 3rd edn. Elsevier Science: Amsterdam, The Netherlands; 1990.
35. Park JY, Paul DR. Correlation and prediction of gas permeability in glassy polymer membrane materials via a modified free volume based group contribution method. J Membr Sci. 1997;125:23–39.
36. Luo S, Liu J, Lin H, Kazanowska BA, Hunckler MD, Roeder RK, Guo R. Preparation and gas transport properties of triptycene-containing polybenzoxazole (PBO)-based polymers derived from thermal rearrangement (TR) and thermal cyclodehydration (TC) processes. J Mater Chem A. 2016;4:17050–62.
37. Hsiao SH, Huang YH. A new class of aromatic polybenzoxazoles containing ortho-phenylenedioxy groups. Euro Polym J. 2004;40:1127–35.
38. Kudo H, Maruyama K, Shindo S, Nishikubo T, Nishimura I. Syntheses and properties of hyperbranched polybenzoxazole by thermal cyclodehydration of hyperbranched poly[o-(t-butoxycarbonyl)amide] via A_2+B_3 approach. J Polym Sci A Polym Chem. 2006;44:3640–9.
39. Hibshman C, Cornelius CJ, Marand E. The gas separation effects of annealing polyimide–hybrid membranes. J Membr Sci. 2003;211:25–40.
40. Zhu H, Ma Y, Fan Y, Shen J. Fourier transform infrared spectroscopy and oxygen luminescence probing combined study of modified sol–gel derived film. Thin Solid Films. 2001;397:95–101.
41. Fina A, Tabuani D, Carniato F, Frache A, Boccaleri E, Camino G. Polyhedral oligomeric silsesquioxanes (POSS) thermal degradation. Thermochim Acta. 2006;440:36–42.
42. Smaïhi M, Jermoumi T, Marignan J, Noble RD. Organic-inorganic gas separation membranes: preparation and characterization. J Membr Sci. 1996;116:211–20.
43. Merkel TC, Freeman BD, Spontak RJ, He Z, Pinnau I, Meakin P, Hill AJ. Ultrapermeable, reverse-selective nanocomposite membranes. Science 2002;296:519–22.
44. Merkel TC, Toy LG, Andrady AL, Gracz H, Stejskal EO. Investigation of enhanced free volume in nanosilica-filled poly(1-trimethylsilyl-1-propyne) by ^{129}Xe NMR spectroscopy. Macromolecules. 2003;36:353–8.
45. Japip S, Wang H, Xiao Y, Chung TS. Highly permeable zeolitic imidazolate framework (ZIF)-71 nano-particles enhanced polyimide membranes for gas separation. J Membr Sci. 2014;467:162–74.
46. Nafisi V, Hägg MB. Development of nanocomposite membranes containing modified Si nanoparticles in PEBAX-2533 as a block

copolymer and 6FDA-durene diamine as a glassy polymer. Appl Mater Interfaces. 2014;6:15643–52.
47. Hasebe S, Aoyama A, Tanaka M, Kawakami H. CO_2 separation of polymer membranes containing silica nanoparticles with gas permeable nano-space. J Membr Sci. 2017;536:148–55.
48. Freeman BD. Basis of permeability/selectivity tradeoff relations in polymeric gas separation membranes. Macromolecules. 1999;32:375–80.
49. Robeson LM. Correlation of separation factor versus permeability for polymeric membranes. J Membr Sci. 1991;62:165–85.
50. Robeson LM. The upper bound revisited. J Membr Sci. 2008;320:390–400.
51. Han SH, Misdan N, Kim S, Doherty CM, Hill AJ, Lee YM. Thermally rearranged (TR) polybenzoxazole: effects of diverse imidization routes on physical properties and gas transport behaviors. Macromolecules. 2010;43:7657–67.